Water **2011**, *3*, 235-253; doi:10.3390/w3010235

OPEN ACCESS

water

ISSN 2073-4441
www.mdpi.com/journal/water

Review

Water Radiolysis: Influence of Oxide Surfaces on H_2 Production under Ionizing Radiation

Sophie Le Caër

Institut Rayonnement Matière de Saclay, Service Interdisciplinaire sur les Systèmes Moléculaires et les Matériaux, UMR 3299 CNRS/CEA SIS2M, Laboratoire de Radiolyse, Bâtiment 546, F-91191 Gif-sur-Yvette Cedex, France; E-Mail: sophie.le-caer@cea.fr

Received: 28 December 2010; in revised form: 27 January 2011 / Accepted: 8 February 2011 / Published: 28 February 2011

Abstract: The radiolysis of water due to ionizing radiation results in the production of electrons, $H^{\bullet}$ atoms, $^{\bullet}OH$ radicals, H_3O^+ ions and molecules (dihydrogen H_2 and hydrogen peroxide H_2O_2). A brief history of the development of the understanding of water radiolysis is presented, with a focus on the H_2 production. This H_2 production is strongly modified at oxide surfaces. Different parameters accounting for this behavior are presented.

Keywords: water; radiolysis; ionizing radiation; H_2 production; solid/liquid interface

---

1. Introduction

The discovery of electrolysis dates back to the end of the XVIIIth century. The electrolysis of water is the decomposition of water (H_2O) into dioxygen (O_2) and dihydrogen (H_2) at electrodes due to an electric current being passed through the water. Another pathway to produce dihydrogen is to perform the radiolysis of water. Water radiolysis is the decomposition of water molecules due to ionizing radiation. Usually, this ionizing radiation stems from the decay of radioactive nuclei, beams of accelerated charged particles (electrons, protons…) and from X-ray radiation (with a photon energy greater than 50–100 eV).

Water radiolysis occurs in many situations (radiotherapy [1], radiosterilization [2], sewage treatment [3], food irradiation [4], *etc*.). In many cases, this water radiolysis is affected by solid/liquid interfaces. For example, in water-cooled nuclear reactors, ionizing radiation induces reactions in water and at the solid (fuel cladding)/liquid interface. In the context of the storage and disposal of nuclear

waste, the heterogeneous materials used (concretes, mortars, *etc*.) can trap significant amounts of water. Radiolysis of these trapped water molecules occurs due to the presence of nuclear waste stored in these materials [5]. The formation of radiolytic products such as H_2 or H_2O_2 has to be evaluated for safety reasons, in order to prevent the breaking or the corrosion of the confining matrix.

After a historical survey, the mechanisms accounting for the radiolysis of water will be presented. An emphasis is put on H_2 production and the modifications of H_2 production in radiolysis at water/oxide interfaces are shown.

2. Water Radiolysis: A Brief Historical Survey

Here we present a brief historical survey of the development of understanding of water radiolysis. This review is inspired by [6-9] in which more details can be found.

The path to radiation chemistry (the area involving the chemical effects induced by high-energy ionizing radiation) was opened by the discovery of X-rays by Röntgen in 1895 and of radioactivity by Becquerel in 1896. A few years later, the chemical changes that water undergoes in aqueous solutions of radium salts were reported. In 1902, Giesel was the first to observe the release of dihydrogen and dioxygen from an aqueous solution of radium bromide [10,11]. Marie Curie compared this phenomenon to "an electrolysis without electrodes". In 1909, Kernbaum from the Curie laboratory reported the production of hydrogen peroxide H_2O_2 [12].

Debierne (Photo 1) was the first to hypothesize that the radiolysis of water proceeds through the production of the $H^{\bullet}$ atom and the $^{\bullet}OH$ radical [13]. This concept was not well accepted at that time. As a matter of fact, the steady-state radiolysis seemed to produce only small quantities of products and the idea was that if free radical intermediates were present, the yield of the products should increase as the dose increased. Nevertheless, one century ago, the radiation sources (seldom more than 100 mg of radium) were very weak, and moreover, the detection techniques were not very sensitive. Therefore, mostly qualitative observations and semi-quantitative measurements could be reported.

Photo 1. André Debierne (1874–1949), around 1901.

Radiation chemistry, trying to unravel the mechanism of water radiolysis, was extensively studied during World War II especially under the Manhattan Project in the United States. Milton Burton's group at the University of Chicago (USA) worked on the mechanism of water radiolysis and they

hypothesized that hydrogen atoms and hydroxyl radicals were produced. It was also shown that the $H^{\bullet}$ and $^{\bullet}OH$ radicals convert the molecular products (H_2 and H_2O_2) back to water molecules and that water used in reactors should be very pure to prevent its radiolytic decomposition. The mechanisms found were then explained by A.O. Allen [14].

After World War II, the mechanism of the radiolysis of water focused on the $H^{\bullet}$ and $^{\bullet}OH$ species. It then became clear that the fate of the oxidizing species was satisfactorily described, which was not the case for the reducing species. Two reducing species, labeled as H and H', were used then [15,16]. Czapski and Schwarz [17] and Collinson *et al.* [18] showed, by studying reactions as a function of the ionic strength, that H' had a unit negative charge, leading to the conclusion that this specie was the hydrated electron. Nevertheless, this was only indirect proof. By 1960, several facilities had achieved the possibility to perform pulsed electron radiolysis [19], which is the equivalent of flash photolysis in the field of radiation chemistry. The final confirmation of the presence of a solvated electron—through observation of its transient absorption spectrum—by means of pulse radiolysis arose in 1962 from Hart and Boag's experiments [20,21], even if Keene may have observed it first [22]. The authors detected a real transient optical absorption around 700 nm and the analogy of the spectrum to that of the electron in ammonia convinced them that it was the solvated electron [20,21]. It is worth stressing that the presence of the solvated electron had been theoretically invoked by Stein in 1952 [23], by Platzman in 1953 [24] and by Weiss in 1953 [25] and 1960 [26].

As time goes by, units and notation changes. At the beginning of radiation chemistry, the notation *M/N* was introduced to quantitatively measure the effect of ionizing radiation, where *M* is the number of molecules transformed and *N* is the number of ion pairs formed. This notation arose from work on gases. At a conference in Leeds in 1952, Milton Burton suggested to replace this *M/N* notation by a radiolytic yield labeled as a "*G* value" which represents the number of molecules created or destroyed per 100 eV of energy deposited in the system [27]. This notion of radiolytic yield *G* is still widely used today. The units have evolved: the SI unit for the dose is now the gray (Gy), which represents 1 joule per kilogram and radiolytic yields are now expressed in mol J^{-1}.

In 1948, Bonet-Maury and Lefort showed that α-rays produced hydrogen peroxide independent of the dissolved dioxygen concentration whereas this hydrogen peroxide yield depended strongly on the dioxygen concentration in the case of X-ray irradiation [28]. This and other results [14] demonstrated the influence of the original ionization density on the molecular yield. Allen suggested that the molecular yield arose from hydrogen atoms and hydroxyl radical recombinations occurring in tiny regions of high radical concentrations [14]. Radicals escaping these regions would diffuse and react with a solute or become distributed more uniformly [14]. Magee [29] and Samuel and Magee [30] expressed a diffusion theory, taking into account this non-homogeneous behavior of ionizing radiation. They used the term of "spur" to characterize a cluster of reactive species. The first complete deterministic treatments of the radiolysis of water addressed specifically the evolution of the molecular yields as a function of the solute concentration [31]. This heterogeneity of the distribution of water decomposition products around the path of the particles (which is called the track) is reflected by the linear energy transfer (LET) value corresponding to the energy deposited by an ionizing particle in the medium per unit path length (LET = −dE/dx). Low-LET radiation (gamma radiation, accelerated electrons, high-energy X-rays) deposits energy discretely along the path of the particles whereas high-LET radiation (heavy ions, alpha particles and neutrons) deposits it densely. Gamma radiation of

^{60}Co has thus a LET value of 0.2–0.3 keV μm^{-1} whereas the value is 140 keV μm^{-1} in the case of 5.3 MeV alpha particles (^{210}Po) [8]. The LET is one of the important parameters to account for the yields of products obtained in radiolysis.

After the 1950s, the development of nuclear reactors enabled more and more radionuclides to be produced. Among them, ^{137}Cs and ^{60}Co sources made it possible to get clean sources of radiation (γ-radiation, and not a mixture of different types of radiation leading to complex chemistry) with high dose rates and high penetrating power enabling the rapid development of radiation chemistry studies. Moreover, starting from 1960, much experimental work was carried out to develop pulse radiolysis equipment to directly measure the time dependence of some of the reactive species formed and the corresponding rate constants. In 1960, pulse radiolysis facilities had a time resolution of the order of the microsecond [19]. The time resolution was then lowered to the nanosecond [32] and then picosecond time scale [33-38]. Among the species to be studied, the hydrated electron [39-42] and the $^{\bullet}$OH radical [43] have received most attention. These transient species are detected by different techniques: optical absorption (mainly in the UV-Visible, more recently in the infrared), conductivity, electron paramagnetic resonance, and so on. The theory is now well established [44,45].

3. Mechanism of Water Radiolysis

The framework in which water radiolysis occurs is now well understood experimentally as well as theoretically [44,45].

Water radiolysis can be written as (1):

$$H_2O \xrightarrow{Ionizing Radiation} e_{aq}^{-}, HO^{\bullet}, H^{\bullet}, HO_2^{\bullet}, H_3O^{+}, OH^{-}, H_2O_2, H_2 \quad (1)$$

The $HO_2^{\bullet}$ radical is a minor (and negligible) species in the case of low-LET radiation. We point out that the dioxygen O_2 is not a primary species in the radiolysis of water.

3.1. The Three Stages

Typically, the radiolytic events occur in three main stages taking place on different typical time scales:

(1) The *physical stage*, which is achieved about 1 fs after the initial matter-ionizing radiation interaction, consists in energy deposition followed by fast relaxation processes. This leads to the formation of ionized water molecules (H_2O^+), excited water molecules (H_2O^*) and sub-excitations electrons (e^-).

(2) During the *physico-chemical stage* (10^{-15}–10^{-12} s), numerous processes occur, including ion-molecule reaction (2), dissociative relaxation (3), autoionization of excited states, thermalization of subexcitation electrons (solvation of electrons) (4), hole diffusion, *etc*.

$$H_2O^{+} + H_2O \rightarrow H_3O^{+} + HO^{\bullet} \quad (2)$$

$$H_2O^{*} \rightarrow HO^{\bullet} + H^{\bullet} \quad (3)$$

$$e^- \rightarrow e^-_{aq} \tag{4}$$

(3) During the *chemical stage* (10^{-12}–10^{-6} s), the species react in the tracks and then diffuse in solution. They can thus react with each other and also with surrounding molecules (in the solute). The track of the particles expands because of the diffusion of radicals and their subsequent chemical reactions. Recombination becomes unimportant after *ca*. 1 μs for low-LET radiation.

These three stages are summarized on Scheme 1.

Scheme 1. Main reactions occurring during the three stages of water radiolysis.

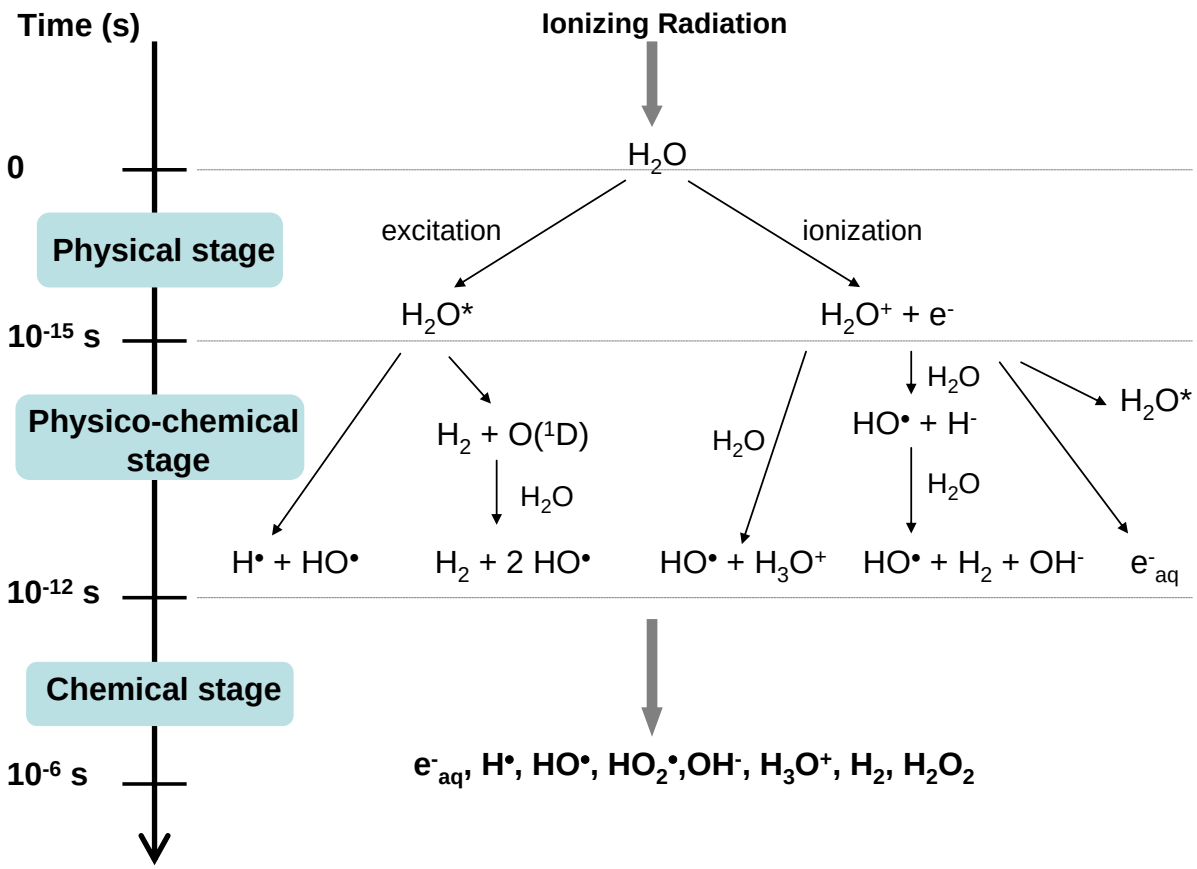

3.2. Radiolytic Yields

Hydrated electrons and hydrogen atoms are strong reducing agents with standard potentials E (H_2O/e^-_{aq}) = −2.9 V_{NHE} and E ($H^+/H^\bullet$) = −2.3 V_{NHE}., respectively. These free radicals can then readily reduce dissolved metal ions to their lower oxidation states. In contrast, hydroxyl radicals are very strong oxidative species with a standard potential E ($HO^\bullet/H_2O$) = +2.7 V_{NHE}.

The radiolytic yields of the different products obtained are known. Nevertheless, these reaction yields depend on time (from initial yields at 1 ps to escape yields at 1 μs after the initial energy deposition). Some escape yields (*G*-values in μmol J^{-1}) obtained experimentally are listed in Table 1 [45,46].

Table 1. Radiolytic yields (in μmol J^{-1}) obtained as a function of the type of radiation and the pH. Gamma radiation and accelerated electrons have a LET value of 0.2–0.3 keV μm^{-1}, whereas in the case of 5.3 MeV alpha particles (^{210}Po) the LET value is 140 keV μm^{-1}.

Radiation	e^-_{aq}	$^{\bullet}OH$	$H^{\bullet}$	H_2	H_2O_2	$HO_2^{\bullet}$
γ Electrons (0.1–10 MeV) pH = 3–11	0.28	0.28	0.06	0.047	0.073	0.0027
γ Electrons (0.1–10 MeV) pH = 0.5	0	0.301	0.378	0.041	0.081	0.0008
5.3 MeV α particles (^{210}Po) pH = 0.5	0	0.052	0.062	0.163	0.150	0.011

The escape yields (Table 1) depend on several parameters, such as the LET of the radiation and the pH [46]. For instance, at a low pH, the H^+ ions capture e^-_{aq} in the spurs leading to the formation of $H^{\bullet}$ atoms. The radiolytic yields of the molecular products (H_2 and H_2O_2) increase with the LET while those of the radicals (e_{aq}^-, $H^{\bullet}$ and $^{\bullet}OH$) decrease as a result of an increase of the density of ionizations in the tracks. Thus, radicals recombine more efficiently with high LET particles (intratrack radical processes becoming increasingly important) favoring the formation of molecular species [47].

Continuous irradiation by low-LET radiation is known to lead to very low steady-state concentrations of dihydrogen and hydrogen peroxide (and the values presented in Table 1 are maximum values) whereas high LET radiation can form significant amounts of these products. The mechanism accounting for this behavior has been proposed by Allen [14,48]. Reactions (5) and (6) make up a chain reaction in which water molecules are formed again; the rate of destruction of H_2 and H_2O_2 is equal to their production rate in water. This chain reaction is propagated by the $H^{\bullet}$ atom and the $^{\bullet}OH$ radical. Therefore, the higher their concentration, the more efficient their recombination.

$$HO^{\bullet} + H_2 \longrightarrow H_2O + H^{\bullet} \tag{5}$$

$$H^{\bullet} + H_2O_2 \longrightarrow H_2O + HO^{\bullet} \tag{6}$$

In the case of low-LET radiation, these reactions are of significant importance in pure water if it is irradiated in a closed system (*i.e.*, H_2 cannot escape from the liquid water phase) or if aqueous systems are irradiated under high dihydrogen pressure. It is worth pointing out that an excess of dihydrogen is dissolved in the primary coolant water of pressurized water reactors (PWRs) in order to prevent the accumulation of oxidant products (such as dioxygen and hydrogen peroxide) responsible for the corrosion of the primary system. However, in practice, dissolved dioxygen or impurities will scavenge the radical species before they convert much of H_2 and H_2O_2 back to water. In the case of high-LET radiation, the chain reaction is no more efficient, as the concentration of the radical species ($H^{\bullet}$ and $^{\bullet}OH$) is too low. Therefore, significant amounts of molecular products are detected. Indeed, it has been shown that water decomposition by radiolysis in the presence of H_2 is a threshold phenomenon as a function of the LET of the radiation [49,50].

3.3. Main Reactions

Some rate constants of the main reactions occurring when the tracks expand are listed in Table 2 [51].

Table 2. A few rate constants used in the description of water radiolysis.

Reaction	Rate constant (10^{10} mol^{-1} dm^3 s^{-1})
$e^-_{aq} + e^-_{aq} + 2H_2O \rightarrow H_2 + 2OH^-$	0.55
$e^-_{aq} + H^\bullet + H_2O \rightarrow H_2 + OH^-$	2.50
$H^\bullet + H^\bullet \rightarrow H_2$	0.78
$e^-_{aq} + HO^\bullet \rightarrow OH^-$	3.00
$e^-_{aq} + H_3O^+ \rightarrow H^\bullet + H_2O$	2.30
$HO^\bullet + HO^\bullet \rightarrow H_2O_2$	0.55
$HO^\bullet + H^\bullet \rightarrow H_2O$	2.00
$H_3O^+ + OH^- \rightarrow 2H_2O$	14.0

The first three reactions in Table 2 are responsible for most of the formation of H_2, *i.e.*, around 70% of the observed yield in the γ radiolysis of water [52,53]. In this latter case, as the hydrogen atom yield is much smaller than that of the hydrated electron (see Table 1), most of the H_2 produced is due to the reaction between two hydrated electrons. Moreover, recent studies have proven that the remainder of the H_2 formation is due to the precursor of the hydrated electron [53]. It has been suggested that the mechanism responsible is the dissociative recombination of the water cation and a non-hydrated electron [53,54].

4. Water Radiolysis and H_2 Production in Heterogeneous Systems at Oxide/Water Interfaces

The radiolysis of water can be strongly affected at solid/liquid interfaces. In heterogeneous systems, all the three stages described in Section 3.1 can be modified with respect to those taking place in bulk water. The energy deposition is different and various energy transfer processes can occur between the initial ionizing radiation-matter interaction and the chemical events observed in water. These phenomena can correspond to a change in the dose received by the system or to a change in initial radiolytic yields. Moreover, the reaction and diffusion of species can be modified by the presence of a solid phase during the chemical stage. All these phenomena are particularly salient when nanoporous materials with large specific surfaces are used (more than 50 m^2/g), as specific interfacial phenomena can thus be revealed.

First studies evidenced the fact that the decomposition of pentane was enhanced in the presence of silicagel [55]. Moreover, the decomposition of azoethane adsorbed on different oxides was proven to depend on the band gap of the oxide [56]. On insulators, an important decomposition was observed, which was not the case when azoethane was adsorbed on semiconductors. These studies demonstrated that an energy transfer from the solid to the adsorbed liquid could take place depending on the band gap of the considered oxide. The term “energy transfer” [56,57] was used by Allen *et al.* to describe the decomposition of the adsorbates. We point out that high-energy radiation is able to excite the solid,

inducing then chemistry in remote regions due to energy transfer from the solid to adsorbed molecules at the surface. This can be considered as "radiation catalysis".

In the case of the radiolysis of water at oxide/water interfaces, numerous studies have focused on H_2 production. These fundamental works have many practical implications. For instance, in nuclear reactors or in stainless steel storage containers with wet nuclear waste materials, water/solid interfaces are numerous and are submitted to ionizing radiation. It is then of significant importance to quantify the H_2 production, as dihydrogen is potentially explosive.

4.1. Modification of H_2 Radiolytic Yields in Heterogeneous Oxide/Water Systems

It was found that the type of oxide greatly impacts the H_2 production [58-62]. This is illustrated in the work of Petrik *et al.*, who studied the H_2 yield as a function of the band gap of different oxides (Figure 1) submitted to γ radiation with adsorbed water molecules at their surface [60]. We point out that the yields are determined with respect to the energy deposited directly by γ-rays to the water molecules adsorbed on oxides. If the H_2 yield thus calculated is greater than the value obtained in bulk water, then an energy transfer from the oxide to water is to be expected. This study enabled the authors to sort oxides into three groups [60]: (i) oxides lowering the H_2 yield as compared to bulk water (CuO, MnO_2...); (ii) oxides that do not seem to affect the H_2 yield (SiO_2, CeO_2, Al_2O_3, TiO_2...), and (iii) oxides increasing the H_2 yield (ZrO_2, Nd_2O_3...). Figure 1 exhibits a resonant maximum for a band gap of the oxide of 5 eV corresponding to the energy of the H-OH bond in a water molecule (5.1 eV). The resonant character of the H_2 yield as a function of the band gap of the oxide is consistent with an exciton transfer mechanism [60]. Zirconia is thus found to produce high amounts of H_2 (Figure 1) [60], which is due to the scavenging of excitons by adsorbed water molecules, as also shown by thermostimulated luminescence experiments.

Nevertheless, other H_2 yields using the same oxides are reported in the literature [61,62]. These differences arise from the origin of the oxide, the size of the particles, *etc*. However, there is a general agreement on the fact that the H_2 yield decreases as the particle size increases [60,63]. We point out that relatively high H_2 yields (as compared to bulk water) are reported, which is not consistent with the known limits for the yield of ionization events, and thus requires the presence of another species that is not ionized.

Figure 1. Dihydrogen yield as a function of the oxide band gap in the γ-radiolysis of H_2O molecules adsorbed on oxides. $G(H_2)$ is calculated with respect to the energy of γ rays directly absorbed by the H_2O molecules. Three groups of oxides are depicted: i) oxides from Group 1 lowering the H_2 yield; (ii) oxides from Group 2 with H_2 yields close to those obtained in bulk water and (iii) oxides from Group 3 increasing the H_2 yield as compared with water radiolysis without oxides. (Reprinted with permission from Ref. [60] Copyright 2001, American Chemical Society).

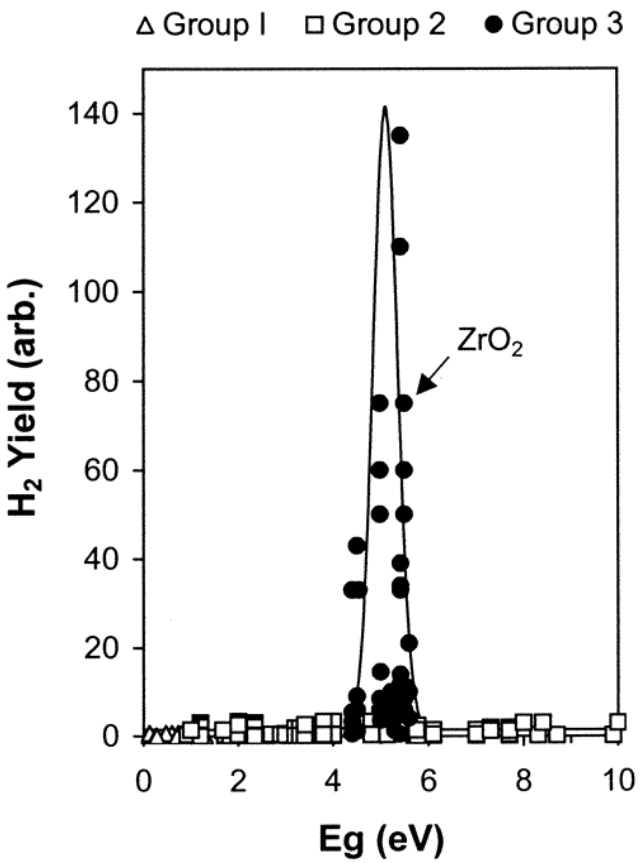

4.2. Mechanisms Accounting for H_2 Production in Oxide/Water Systems

Generally, radiation energy absorbed by solids dissipates into three main channels: thermal, defect formation and luminescence. Thus, irradiation of oxides may give rise to color centers that absorb in the UV and visible range. For instance, in SiO_2, UV-absorbing color centers are associated with trapped electrons and visible color centers are associated with hole trapping on impurities. For disperse systems, an additional channel, namely surface reactions, is opened. In heterogeneous systems, there is a competition between surface reactions and the other energy dissipation channels.

In an irradiated heterogeneous system, when the two phases each constitute a significant fraction of the total mass, the ionizing energy is absorbed significantly by both phases. After the absorption of a high-energy photon, a high energy Compton electron is ejected. This electron induces a large number of secondary electrons of energies in the 100 eV range. As charge carriers may cross from one phase to the other one, phenomena are thus different from those observed in a homogeneous phase.

The processes underlying the dihydrogen production at oxide/water interfaces can be described as follows. The interaction of radiation with an oxide causes electronic excitations, which promote an electron from the valence band to the conduction band, leaving a hole in the valence band (7).

$$M \xrightarrow{radiation} e^- + h^+ \tag{7}$$

When an excited electron and a hole in the valence band remain bound together by Coulomb interactions, they are referred to as an exciton. The energy of the exciton is a little lower than the band gap energy. In semiconductors, the energy transfers by the coherent excitons. Similarly to electrons and holes, excitons can be self-trapped in insulators. They can self-trap in BeO, SiO_2, GeO_2, MgO, Li_2O and other oxides due to strong exciton-lattice interaction [64-66]. We point out that the self-trapping of excitons does not occur in MgO, CaO nor in semiconductors [64]. The formation of self-trapped excitons (STE) has two consequences: the localization of the excitation energy and the creation of highly distorted sites (structural irregularities in terms of bond length and bond angle).

Among all the oxides of interest, the most extensive work has been performed on silica, due to the development of high-purity silica for optical fiber applications. Therefore, the electronic excitation and defect formation in silica are well understood. In silica, the relaxation of singlet excitons to the triplet state and the adiabatic localization of the triplet excitons occurs rapidly and gives rise, within ≈250 fs, to the self trapped excitons (STE) in the triplet state [67], see Equation 8. Calculations evidence that there is no barrier for self-trapping [68].

$$^1exciton \longrightarrow {}^3STE \tag{8}$$

Calculations have also proven that the exciton self-trapping is accompanied by a weakening of one of the two Si-O bonds with an oxygen atom and by a small displacement of the oxygen ion towards an interstitial position [69]. This species resembles an E' center (≡Si$^\bullet$, with ≡ standing for the three bonds established by the silicon atom with oxygen atoms)–peroxy linkage (≡Si-O-O-Si≡) defect pair. Further adiabatic displacement of the interstitial oxygen atom to a more distant potential minimum results in the formation of a permanent Frenkel defect pair [69]. Experiments clearly show that certain types of damage in amorphous silica involve STEs [70]. In about 1% of the STE states created, the decay channel back to the electronic ground state leads to a damage state. Different defects are believed to be formed by the action of a single STE, or by the interaction of multiple STEs. In the case of amorphous silica subject to proton irradiation, Matsunami and Hosono have demonstrated that the Frenkel defect is created by nonradiative decay of two neighboring self-trapped excitons generated through O 2s-shell ionization followed by an Auger decay process [71]. Lastly, interstitial O_2 molecules are detected upon irradiation of silica [72,73]. One of the possible mechanisms of O_2 formation in irradiated silica stems from the reaction between two peroxy linkages (≡Si-O-O-Si≡) [72,74].

It has been suggested [75] that the free exciton in hydroxylated silica, prior to its self-trapping, reacts with the surface hydroxyl groups, leading to the breakage of the O-H bond (9). The ≡SiO$^\bullet$ radicals have indeed been detected by EPR (Electron Paramagnetic Resonance) spectroscopy [76,77]. Moreover the H$^\bullet$ atom has been observed upon radiolysis of fused silica [78], MCM-41 mesoporous [79] and Vycor glasses [80]. This exciton reactivity at the surface is in competition with the subpicosecond exciton relaxation and the self-trapping processes. Different trapping sites are possible: silanols (labeled as ≡SiOH) (9) or physisorbed water molecules (10). It has been shown that

silanol groups are much less efficient at producing H_2 than adsorbed water molecules [81]. We point out that the direct excitation of hydroxyl groups, which are present as impurities on the silica surface, is negligible. The division of bulk silica into nanometric particles emphasizes the role played by the surface. This dramatic surface effect is then gradually suppressed when the size of the silica particles is increased.

$$^{3}exciton + \equiv SiOH \longrightarrow \equiv SiO^{\bullet} + H^{\bullet} \tag{9}$$

$$^{3}exciton + H_2O \longrightarrow HO^{\bullet} + H^{\bullet} \tag{10}$$

Nevertheless, the hydroxylation of the silica surface has an effect on the nature of the mechanism and a strongly dehydrated surface can tune the excitonic chemistry to a more ionic one as shown by the reactivity of the electron at the surface (dissociative electron attachment to -OH groups (11)) [82]. The reaction shown in Equation 11 accounts for the previous observation of ionic reactions on high temperature activated silica surfaces [83]. This variation of the surface chemistry originates from the modulation of the hydroxyl content which is present as an impurity in the band gap.

$$e^{-} + \equiv SiOH \longrightarrow \equiv SiO^{-} + H^{\bullet} \tag{11}$$

Contrary to silica for which mostly excitonic chemistry is reported, both zeolites and γ-alumina (Al_2O_3) exhibit an ionic surface chemistry [84]. In the case of zeolites, a very efficient charge separation takes place due to the presence of Na^+ and water clusters which are electron-trapping sites [85]. In the case of alumina, both electrons and holes migrate to the surface. It is suggested that positive holes rapidly react with surface –OH groups to give H^+ (12):

$$h^{+} + -OH \rightarrow -O^{\bullet} + H^{+} \tag{12}$$

The protons will then react with trapped electrons (e_t^-) at the surface to generate $H^{\bullet}$ atom (13):

$$H^{+} + e_t^{-} \rightarrow H^{\bullet} \tag{13}$$

Whether ionic or excitonic chemistry, the resulting $H^{\bullet}$ atoms dimerize forming H_2 (14).

$$H^{\bullet} + H^{\bullet} \longrightarrow H_2 \tag{14}$$

4.3. The Fate on Electrons and Holes—A Textbook Case: Silica

Due to the scattering of light in heterogeneous systems, few studies have focused on the electron, although it is a precursor of dihydrogen (see Table 2). However, it was shown in the case of zeolites that the electron spectrum in the cavities of the zeolites strongly depends on the water loading [85]. A red spectral shift of this spectrum with the decreasing size of the confined water clusters was observed and attributed to a decreased solvation of the electron and an increased delocalization [85]. Moreover, pulse radiolysis experiments of aqueous suspensions of nanometer-sized silica have proven that electrons formed in the particle migrate out in the bulk water [86]. Energy is deposited in silica, crosses the solid-liquid interface and appears in the aqueous phase as solvated electrons (15) [86].

$$e^{-} + nH_2O \longrightarrow e_{aq}^{-} \tag{15}$$

Holes, on the other hand, remain trapped in the silica particles [87]. Thus, the dihydrogen produced in these colloidal silica suspensions may only be due to the energy deposited in the liquid phase or to reactions at the particle surface.

More recently, Monte-Carlo simulations of electron transport through a silica-water system were performed in order to better understand the physical and physico-chemical stages observed in water confined in an array of cylindrical pores made of amorphous silica [88]. The respective energy levels in water and in silica are presented in Figure 2 [88].

Figure 2. Scheme of the energy levels in water and in silica. The conduction band edges with respect to the vacuum level are taken as V_0 (H_2O) = −1.2 eV and V_0 (SiO_2) = −0.9 eV, respectively. The difference between the valence and conduction band edge is 9.0 eV in silica and 8.7 eV in water. (Reprinted with permission from Ref. [88] Copyright 2010, American Chemical Society).

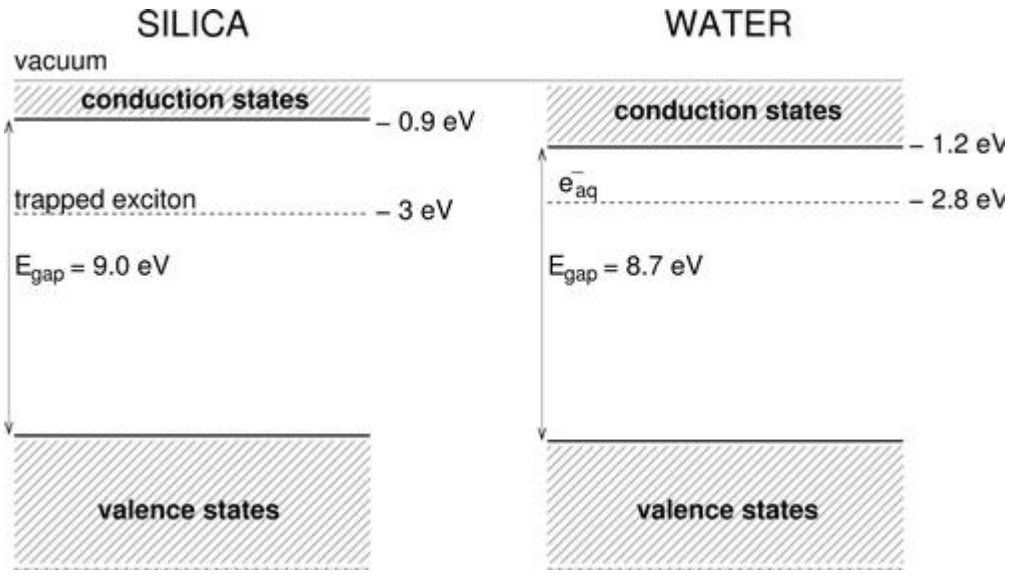

Ouerdane *et al.* have shown that the presence and solvation of a large excess of electrons in water is controlled exclusively by the difference between the conduction band edge of the materials ΔU ($\Delta U = V_0$ (SiO_2) − V_0 (H_2O) = 0.3 eV) [88]. If this energy difference is greater than the thermal energy, then the electrons are trapped in water, where they thermalize and get solvated. This phenomenon can in principle be observed for any material for which the ΔU value is high enough [88].

Ouerdane *et al.* have also calculated the yields of the hydrated electron at the end of the physico-chemical stage for different porosities (Figure 3) [88]. The electron yields increase as the pore size decreases, especially below 100 nm (Figure 3). This yield depends on the relative value of the low-energy electron mean free path in silica with respect to the pore radius and to the porosity. For very small pores, the electron yields do not depend on the porosities reported for which the volume of water and the volume of silica are similar (Figure 3). For very large pores, the difference in the electron yields is linked to the difference in the water fraction of the simulation cell for the two porosities, as the surface crossing by electrons becomes negligible.

The simulations of Ouerdane *et al.* are in agreement with the experimental work of Schatz *et al.* [86]. The low-energy electrons produced in silica cross the silica-water interface to be

trapped in water when their diffusion length becomes comparable to the particle size. This effect becomes extremely efficient for small particles (below 10 nm). After that, these electrons will diffuse and influence the fate of the water radiolysis.

Figure 3. Yields of the hydrated electron as a function of the pore radius for two porosities: 0.5 (considered as the reference, circles) and 0.7 (crosses) calculated at the end of the physico-chemical stage. The porosity is defined as the volume occupied by water in cylindrical pores divided by the total volume of the simulation cell. (Reprinted with permission from Ref. [88] Copyright 2010, American Chemical Society).

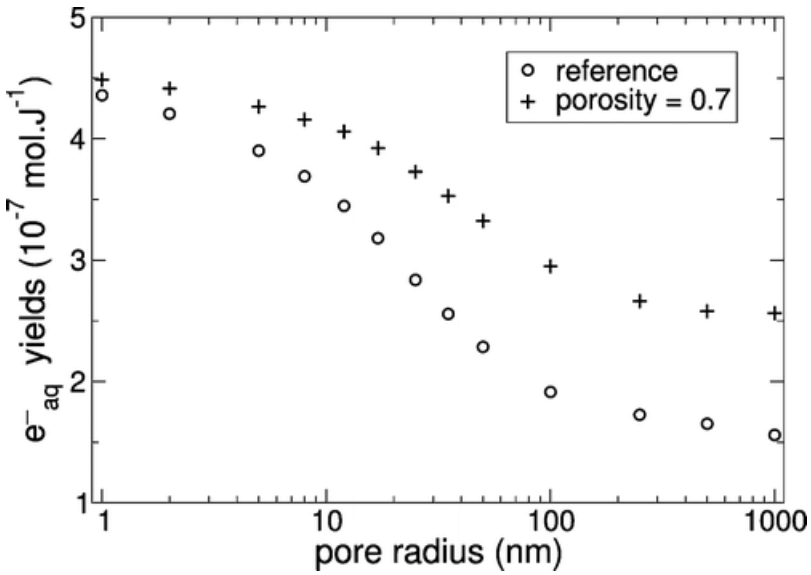

4.4. Parameters Affecting the Dihydrogen Yield

Many parameters have been found to affect the dihydrogen yield at the oxide/water interface:

- the band gap of the oxide (Figure 1) [60];
- the doping of the oxide [60];
- the crystal phase [89];
- the exciton migration distance. Higher distances favor exciton exciton recombination or self-trapping instead of their reaction at the interface [90];
- The water adsorption form (physisorbed/chemisorbed water) [81]. The measure of H_2 production from 10 MeV-electron irradiation on mesoporous silica has shown that adsorbed water (physisorbed water) is attacked preferentially. Silanol groups (chemisorbed water) are only attacked when they are in majority with respect to adsorbed water. However, they are much less efficient in producing H_2 [81];
- the surface density of hydroxyl groups. The higher the density of trapping sites, the more efficient is the energy transfer. However, we point out that not all hydroxyl groups are efficient trapping sites. Hydroxyl groups with strong hydrogen bonds are not very efficient trapping sites [81,90];

- the dose rate of the irradiation. In the case of high dose rate irradiation, the H_2 yields are much smaller than in the case of γ-irradiation with low dose rate; most of the received energy is not used for H_2 production but for recombination of excitons on defect sites (cathodoluminescence) or exciton-exciton reaction [90]. The accumulation of defects under irradiation can provide an additional deactivation pathway for excitons [91]: this is indeed the principle of cathodoluminescence spectroscopy [92]. Therefore, less excitons can reach the surface to induce H_2 production and the dihydrogen yields are then strongly decreased [90];
- the LET value of the particles. Contrary to the phenomena described in the bulk phase, the H_2 yields for water adsorbed on zirconia were found to exhibit a marked decrease in the case of 5 MeV helium ion radiolysis as compared to γ-radiolysis. The heavy ions induce the formation of much more Frenkel defects in zirconia than the γ-radiolysis, which prevents the excitons from migrating to the surface [93].

4.5. Modification of Kinetics upon Confinement

In the studies of oxide/water heterogeneous systems, nanoporous materials, which have a high surface/volume ratio favoring the interface phenomena, have been widely used. Large effects on kinetics are thus expected due to restricted motion. It is usually considered that the intrapore encounter probability is increased, which accelerates reactions. However, the situation is more complex. It is thus important to point out that the H_2 production was measured in nanoporous silica/water systems without the presence of any scavengers [62,90]. In the case of bulk water, almost no H_2 is produced in the absence of scavengers. Therefore, the reaction involving the destruction of H_2 by $HO^{\bullet}$ in free and pure water (Reaction 5) does not occur in confined water. In these systems, the diffusion is limited and the interpore encounter probability between H_2 and $HO^{\bullet}$ is decreased. Compartmentalization effects prevail here, decreasing the interpore diffusion coefficients of the reactive species.

5. Conclusions

Since the beginning of radiation chemistry at the end of the XIXth century, much work has been devoted to unraveling the mechanisms of water radiolysis. These mechanisms, leading to the formation of radical species ($H^{\bullet}$, $^{\bullet}OH$, e^{-}_{aq}) and molecular products (H_2, H_2O_2) are now well understood. The radiolysis of water in contact with oxide surfaces is of significant practical importance but is much more complex. Higher H_2 yields (as compared to bulk water) can be measured, demonstrating that a very efficient energy transfer can take place at the interface. Many parameters control this energy transfer, for instance the oxide band gap, the water adsorption form, and the energy migration distance. Nevertheless, the understanding of the phenomena happening during water radiolysis in heterogeneous media is not complete, and the theoretical framework has to be more firmly established.

In conclusion, the chemistry induced by ionizing radiation at the oxide/adsorbate interface has many practical applications (transformation or decay of pollutants for example). Therefore, there is a need to fundamentally understand the radiolytic processes occurring on oxide surfaces.

References

1. Schmid, T.E.; Dollinger, G.; Hable, V.; Greubel, C.; Zlobinskaya, O.; Michalski, D.; Molls, M.; Roeper, B. Relative biological effectiveness of pulsed and continuous 20 MeV protons for micronucleus induction in 3D human reconstructed skin tissue. *Radiother. Oncol.* **2010**, *95*, 66-72.
2. Maquille, A.J.; Jiwan, J.L.H.; Tilquin, B. Radiosterilization of drugs in aqueous solutions may be achieved by the use of radioprotective excipients. *Int. J. Pharm.* **2008**, *349*, 74-82.
3. Guo, Z.B.; Tang, D.Y.; Liu, X.G.; Zheng, Z. Gamma irradiation-induced Cd^{2+} and Pb^{2+} removal from different kinds of water. *Rad. Phys. Chem.* **2008**, *77*, 1021-1026.
4. Katayama, T.; Nakauma, M.; Todoriki, S.; Phillips, G.O.; Tada, M. Radiation-induced polymerization of gum arabic (Acacia senegal) in aqueous solution. *Food Hydrocolloid.* **2006**, *20*, 983-989.
5. Bouniol, P.; Bjergbakke, E. A comprehensive model to describe radiolytic processes in cement medium. *J. Nucl. Mat.* **2008**, *372*, 1-15.
6. *Early Developments in Radiation Chemistry*; Kroh, J., Ed.; Royal Society of Chemistry: Cambridge, UK, 1989.
7. Jonah, C.D. A short history of the radiation chemistry of water. *Radiat. Res.* **1995**, *144*, 141-147.
8. Ferradini, C.; Jay-Gerin, J.P.; La radiolyse de l'eau et des solutions aqueuses: historique et actualité. *Can. J. Chem.* **1999**, *77*, 1542-1575.
9. Zimbrick, J.D. Radiation research society 1952–2002 Radiation chemistry and the Radiation Research Society: A history from the beginning. *Radiat. Res.* **2002**, *158*, 127-140.
10. Giesel, F. Uber Radium und radioactive Stoffe. *Ber. Dtsch. Chem. Ges.* **1902**, *35*, 3608-3611.
11. Giesel, F. Uber den Emanationskörper aus Pechblende. *Ber. Dtsch. Chem. Ges.* **1903**, *36*, 342-347.
12. Kernbaum, M. Sur la décomposition de l'eau par les rayons béta du radium et par les rayons ultra-violets. *Le Radium* **1909**, *6*, 225-228.
13. Debierne, A. Recherches sur les gaz produits par les substances radioactives. Décomposition de l'eau. *Ann. Phys. (Paris)* **1914**, *2*, 97-127.
14. Allen, A.O. Radiation chemistry of aqueous solutions. *J. Phys. Colloid Chem.* **1948**, *52*, 479-490.
15. Barr, N.F.; Allen, A.O.; Hydrogen atoms in the radiolysis of water. *J. Phys. Chem* **1959**, *63*, 928-931.
16. Hayon, E.; Allen, A.O. Evidence for two kinds of "H atoms" in the radiation chemistry of water. *J. Phys. Chem.* **1961**, *65*, 2181-2185.
17. Czapski, G.; Schwarz, H.A. The nature of the reducing radical in water radiolysis. *J. Chem. Phys* **1962**, *66*, 471-474.
18. Collinson, E.; Dainton, F.S.; Smith, D.R.; Tazuké, S. Evidence for the unit negative charge on the "hydrogen atom" formed by the action of ionising radiation on aqueous systems. *Proc. Chem. Soc.* **1962**, 140-141.
19. Keene, J.P. Kinetics of radiation-induced chemical reactions. *Nature* **1960**, *188*, 843-844.
20. Hart, E.J.; Boag, J.W. Absorption spectrum of the hydrated electron in water and in aqueous solutions. *J. Am. Chem. Soc.* **1962**, *84*, 4090-4095.
21. Boag, J.W.; Hart, E.J. Absorption spectra in irradiated water and some solutions. *Nature* **1963**, *197*, 45-47.

22. Keene, J.P. Optical absorption in irradiated water. *Nature* **1963**, *197*, 47-48.
23. Stein, G. Some aspects of the radiation chemistry of organic solutes. *Disc. Faraday Soc.* **1952**, *12*, 227-234.
24. Platzman, R.L. *Physical and Chemical Aspects of Basic Mechanisms in Radiobiology*; Magee, J.L., Kamen, M.D., Platzman, R.L., Eds.; National Research Council: Washington, DC, USA, 1953; p. 22.
25. Weiss, J. Radiation chemistry. *Annu. Rev. Phys. Chem.* **1953**, *4*, 143-166.
26. Weiss, J. Primary processes in the action of ionizing radiations on water: formation and reactivity of self-trapped electrons ('polarons'). *Nature* **1960**, *186*, 751-752.
27. Burton, M. General discussion. *Disc. Faraday Soc.* **1952**, *12*, 317-318.
28. Bonet-Maury, P.; Lefort, M. Formation of hydrogen peroxide in water irradiated with X- and alpha-rays. *Nature* **1948**, *162*, 381-382.
29. Magee, J.L. Theory of radiation chemistry. I. Some effects of variation in ionization density. *J. Am. Chem. Soc.* **1951**, *73*, 3270-3275.
30. Samuel, A.H.; Magee, J.L. Theory of radiation chemistry. II. Track effects in radiolysis of water. *J. Chem. Phys.* **1953**, *21*, 1080-1087.
31. Schwarz, H.A. Applications of the spur diffusion model to the radiation chemistry of aqueous solutions. *J. Phys. Chem.* **1969**, *73*, 1928-1937.
32. Hunt, J.W.; Thomas, J.K. Pulse-radiolysis studies of the formation of triplet excited states in cyclohexane solutions of naphtalene and anthracene. *J. Chem. Phys.* **1967**, *46*, 2954-2958.
33. Bronskill, M.J.; Hunt, J.W. A pulse-radiolysis system for the observation of short-lived transients. *J. Phys. Chem.* **1968**, *72*, 3762-3766.
34. Bronskill, M.J.; Taylor, W.B.; Wolff, R.K.; Hunt, J.W. Design and performance of a pulse radiolysis system capable of picosecond time resolution. *Rev. Sci. Instrum.* **1970**, *41*, 333-340.
35. Jonah, C.D. A wide-time range pulse radiolysis system of picosecond time resolution. *Rev. Sci. Instrum.* **1975**, *46*, 62-66.
36. Kobayashi, H.; Tabata, Y. A 20 ps time resolved pulse radiolysis using two linacs. *Nucl. Inst. and Meth. Phys. Res. B* **1985**, *10-11*, 1004-1006.
37. Wishart, J.F.; Cook, A.R.; Miller, J.R. The LEAF picosecond pulse radiolysis facility at Brookhaven National Laboratory. *Rev. Sci. Instrum.* **2004**, *75*, 4359-4366.
38. Marignier, J.-L.; de Waele, V.; Monard, H.; Gobert, F.; Larbre, J.-P.; Demarque, A.; Mostafavi, M.; Belloni, J. Time-resolved spectroscopy at the picosecond laser-triggered electron accelerator ELYSE. *Rad. Phys. Chem.* **2006**, *75*, 1024-1033.
39. Bronskill, M.J.; Wolff, R.K.; Hunt, J.W. Picosecond pulse radiolysis studies. I. The solvated electron in aqueous and alcohol solutions. *J. Chem. Phys* **1970**, *53*, 4201-4210.
40. Jonah, C.D.; Matheson, M.S.; Miller, J.R.; Hart, E.J. Yield and decay of the hydrated electron from 100 ps to 3 ns. *J . Phys. Chem.* **1976**, *80*, 1267-1270.
41. Bartels, D.M.; Cook, A.R.; Mudaliar, M.; Jonah, C.D. Spur decay of the solvated electron in picosecond radiolysis measured with time-correlated absorption spectroscopy. *J. Phys. Chem. A* **2000**, *104*, 1686-1691.

42. Muroya, Y.; Lin, M.; Wu, G.; Iijima, H.; Yoshii, K.; Ueda, T.; Kudo, H.; Katsumura, Y. A re-evaluation of the initial yield of the hydrated electron in the picosecond time range. *Rad. Phys. Chem.* **2005**, *72*, 169-172.
43. Jonah, C.D.; Miller, J.R. Yield and decay of the OH radical from 200 ps to 3 ns. *J. Phys. Chem.* **1977**, *81*, 1974-1976.
44. Buxton, G.V. *Radiation Chemistry. Principles and Applications*; Farhataziz, Rodgers, M.A.J., Eds.; Verlag Chemie Publishers: Weinheim, Germany, 1987.
45. Spinks, J.W.T.; Woods, R.J. *An Introduction to Radiation Chemistry*, 3rd ed.; Wiley-Interscience publication: New York, NY, USA, 1990.
46. Ferradini, C.; Jay-Gerin, J.P. The effect of pH on water radiolysis: a still open question. A minireview. *Res. Chem. Intermed.* **2000**, *26*, 549-565.
47. LaVerne, J.A.; Schuler, R.H. Decomposition of water by very high linear energy transfer radiations. *J. Phys. Chem.* **1983**, *87*, 4564-4565.
48. Allen, A.O.; Hochanadel, C.J.; Ghormley, J.A.; Davis, T.W. Decomposition of water and aqueous solutions under mixed fast neutron and gamma radiation. *J. Phys. Chem.* **1952**, *56*, 575-586.
49. Pastina, B.; Isabey, J.; Hickel, B. The influence of water chemistry on the radiolysis of the primary coolant water in pressurized water reactors. *J. Nucl. Mat.* **1999**, *264*, 309-318.
50. Pastina, B.; LaVerne, J.A. Effect of molecular hydrogen on hydrogen peroxide in water radiolysis. *J. Phys. Chem. A* **2001**, *105*, 9316-9322.
51. Buxton, G.V.; Greenstock, C.L.; Helman, W.P.; Ross, A.B. Critical review of rate constants for reactions of hydrated electrons, hydrogen atoms and hydroxyl radicals ($^{\bullet}OH/^{\bullet}O^{-}$) in aqueous solution. *J. Phys. Chem. Ref. Data* **1988**, *17*, 513-531.
52. Pimblott, S.M.; LaVerne, J.A. Stochastic simulation of the electron radiolysis of water and aqueous solutions. *J. Phys. Chem. A* **1997**, *101*, 5828-5838.
53. Pastina, B.; LaVerne, J.A.; Pimblott, S.M. Dependence of molecular hydrogen formation in water on scavengers of the precursor to the hydrated electron. *J. Phys. Chem. A* **1999**, *103*, 5841-5846.
54. LaVerne, J.A.; Pimblott, S.M. New mechanism for H_2 formation in water. *J. Phys. Chem. A* **2000**, *104*, 9820-9822.
55. Caffrey, J.M.; Allen, A.O. Radiolysis of pentane adsorbed on mineral solids. *J. Phys. Chem.* **1958**, *62*, 33-37.
56. Rabe, J.G.; Rabe, B.; Allen, A.O. Radiolysis and energy transfer in the adsorbed state. *J. Phys. Chem.* **1966**, *70*, 1098-1107.
57. Rabe, J.G.; Rabe, B.; Allen, A.O. Radiolysis in the adsorbed state. *J. Am. Chem. Soc.* **1964**, *86*, 3887-3888.
58. Garibov, A.A.; Gezalov, K.B. Velibekova, G.Z.; Ramazanova, M.K.; Kasumov, R.D.; Agaev, T.N.; Gasanov, A.M. Heterogeneous radiolysis of water: effect of the concentration of water in the adsorbed phase on the hydrogen yield. *High Energy Chem.* **1987**, *21*, 416-420.
59. Nakashima, M.; Masaki, N.M. Radiolytic hydrogen gas formation from water adsorbed on type Y zeolites. *Radiat. Phys. Chem.* **1996**, *47*, 241-245.
60. Petrik, N.G.; Alexandrov, A.B.; Vall, A.I. Interfacial energy transfer during gamma radiolysis of water on the surface of ZrO_2 and some other oxides. *J. Phys. Chem. B* **2001**, *105*, 5935-5944.

61. LaVerne, J.A.; Tandon, L. H_2 production in the radiolysis of water on CeO_2 and ZrO_2. *J. Phys. Chem. B* **2002**, *106*, 380-386.
62. Rotureau, P.; Renault, J.P.; Lebeau, B.; Patarin, J.; Mialocq, J.C. Radiolysis of confined water: Molecular hydrogen formation. *Chemphyschem.* **2005**, *6*, 1316-1323.
63. LaVerne, J.A.; Tonnies, S.E. H_2 production in the radiolysis of aqueous SiO_2 Suspensions and Slurries. *J. Phys. Chem. B* **2003**, *107*, 7277-7280.
64. Itoh, N. Self-trapped exciton model of heavy-ion track registration. *Nucl. Inst. and Meth. Phys. Res. B* **1996**, *116*, 33-36.
65. Itoh, C.; Tanimura, K.; Trukhin, A.N. Time-resolved spectroscopic study of self-trapped excitons in germanium oxides. *Nucl. Inst. and Meth. Phys. Res. B* **1996**, *116*, 72-76.
66. Bautin, K.V.; Kudyakov, S.V.; Ogorodnikov, I.N.; Kruzhalov, A.V.; Yakovlev, V.Y. Exciton dynamics and energy transfer in beryllium oxide crystals with defects. *J. Luminesc.* **1998**, *76-77*, 467-469.
67. Saeta, P.N.; Greene, B.I. Primary relaxation processes at the band edge of SiO_2. *Phys. Rev. Lett.* **1993**, *70*, 3588-3591.
68. Isamel-Beigi, S.; Louie, S.G. Self-trapped excitons in silicon-dioxide: mechanism and properties. *Phys. Rev. Lett.* **2005**, *95*, 154601.
69. Shluger, A.; Stefanovich, E. Models of the self-trapped exciton and nearest-neighbor defect pair in SiO_2. *Phys. Rev. B* **1990**, *42*, 9664-9673.
70. Tsai, T.E.; Griscom, D.L. Experimental evidence for excitonic mechanism of defect generation in high-purity silica. *Phys. Rev. Lett.* **1991**, *67*, 2517-2520.
71. Matsunami, N.; Hosono, H. Bi-self trapped-exciton model for Frenkel defect formation in amorphous SiO_2 by proton irradiation. *Phys. Rev. B* **1999**, *60*, 10616-10619.
72. Hosono, H.; Kawazoe, H.; Matsunami, N. Experimental evidence for Frenkel defect formation in amorphous SiO_2 by electronic excitation. *Phys. Rev. Lett.* **1998**, *80*, 317-320.
73. Stevens-Kalceff, M.A. Electron-irradiation-induced radiolytic oxygen generation and microsegregation in silicon dioxide polymorphs. *Phys. Rev. Lett.* **2000**, *84*, 3137-3140.
74. Shluger, A.L.; Gavartin, J.L.; Szymanski, M.A.; Stoneham, A.M. Atomistic modelling of radiation effects: Towards dynamics of exciton relaxation. *Nucl. Inst. and Meth. Phys. Res. B* **2000**, *166-167*, 1-12.
75. Shkrob, I.A.; Trifunac, A.D.; Spin-polarized H/D atoms and radiation chemistry in amorphous silica. *J. Chem. Phys.* **1997**, *107*, 2374-2385.
76. Silin, A.R.; Skuja, L.N. Spectroscopic properties and mutual conversion reactions of quasi-molecular hydroxyl and non-bridging oxygen defects in vitreous silica. *J. Molec. Struct.* **1980**, *61*, 145-148.
77. Griscom, D.L. Defect structure of glasses. *J. Non-Cryst. Solids* **1985**, *73*, 51-77.
78. Griscom, D.L. Thermal bleaching of X-ray-induced defect centers in high purity fused silica by diffusion of radiolytic molecular hydrogen. *J. Non-Cryst. Solids* **1984**, *68*, 301-325.
79. Chemirisov, S.C.; Werst, D.W.; Trifunac, A.D. Formation, trapping and kinetics of H atoms in wet zeolites and mesoporous silica. *Radiat. Phys. Chem.* **2001**, *60*, 405-410.
80. Tarasov, V.F.; Chemerisov, S.D.; Trifunac, A.D. H-atom electron-spin polarization in irradiated water and ice confined in the nanopores of Vycor glass. *J. Phys. Chem. B* **2003**, *107*, 1293-1301.

81. Brodie-Linder, N.; Le Caër, S.; Alam, M.S.; Renault, J.P.; Alba-Simionesco, C. H_2 formation by electron irradiation of SBA-15 materials and the effect of CuII grafting. *Phys. Chem. Chem. Phys.* **2010**, *12*, 14188-14195.
82. Brunet, F.; Charpentier, T.; Le Caër, S.; Renault, J.P. Solid state NMR characterization of a controlled-pore glass and of the effects of electron irradiation. *Solid State Nucl. Magn. Reson.* **2008**, *33*, 1-11.
83. Barter, C.W.; Wagner, C.D. Generation of catalytic activity in silica gel by ionizing radiation. *J. Phys. Chem.* **1964**, *68*, 2381-2383.
84. Thomas, J.K. Physical aspects of radiation-induced processes on SiO_2, gamma-Al_2O_3, zeolites and clays. *Chem. Rev.* **2005**, *105*, 1683-1734.
85. Liu, X.; Zhang, G.; Thomas, J.K. Spectroscopic Studies of Electron and Hole Trapping in Zeolites : Formation of Hydrated Electrons and Hydroxyl Radicals. *J. Phys. Chem. B* **1997**, *101*, 2182-2194.
86. Schatz, T.; Cook, A.R.; Meisel, D. Charge carrier transfer across the silica nanoparticle/water interface. *J. Phys. Chem. B* **1998**, *102*, 7225-7230.
87. Dimitrijevic, N.M.; Henglein, A.; Meisel, D. Charge separation across the silica nanoparticle/water interface. *J. Phys. Chem. B* **1999**, *103*, 7073-7076.
88. Ouerdane, H.; Gervais, B.; Zhou, H.; Beuve, M.; Renault, J.P. Radiolysis of water confined in porous silica: a simulation study of the physicochemical yields. *J. Phys. Chem. C* **2010**, *114*, 12667-12674.
89. LaVerne, J.A. H_2 formation from the radiolysis of liquid water with zirconia. *J. Phys. Chem. B* **2005**, *109*, 5395-5397.
90. Le Caër, S.; Rotureau, P.; Brunet, F.; Charpentier, T.; Blain, G.; Renault, J.P.; Mialocq, J.-C. Radiolysis of confined water: Hydrogen production at a high dose rate. *Chemphyschem.* **2005**, *6*, 2585-2596.
91. Glinka, Y.D.; Lin, S.-H.; Chen, Y.-T. Two-photon-excited luminescence and defect formation in SiO_2 nanoparticles induced by 6.4-eV ArF laser light. *Phys. Rev. B* **2000**, *62*, 4733-4743.
92. Ozawa, L. *Cathodoluminescence, Theory and Applications*; Verlag Chemie Publishers: Weinheim, Germany, 1990.
93. LaVerne, J.A.; Tandon, L. H_2 production in the radiolysis of water on UO_2 and other oxides. *J. Phys. Chem. B* **2003**, *107*, 13623-13628.